Modeling of Modifier-Solute Peak Interactions in Chromatography

Guido Ströhlein and Massimo Morbidelli
Swiss Federal Institute of Technology Zurich, Institut für Chemie- and Bioingenieurwissenschaften, ETH-Hönggerberg/HCI, CH-8093 Zurich, Switzerland

Hyun-Ku Rhee
Seoul National University, School of Chemical Engineering and Institute of Chemical Processes, Gwanak-ku, Seoul, 151-744, Korea, and Swiss Federal Institute of Technology Zurich, Institut für Verfahrenstechnik, Sonneggstrasse 3, CH-8092 Zurich, Switzerland

Marco Mazzotti
Swiss Federal Institute of Technology Zurich, Institut für Verfahrenstechnik, Sonneggstrasse 3, CH-8092 Zurich, Switzerland

DOI 10.1002/aic.10624
Published online October 4, 2005 in Wiley InterScience (www.interscience.wiley.com).

The behavior of a chromatographic column where a single solute is fed in the presence of a suitable modifier is analyzed in the context of equilibrium theory. In particular, the pulse propagation of the solute, whose retention depends on the modifier concentration, has been analyzed as a full-fledged binary problem by the method of hodograph transformation applied to the pair of quasilinear differential equations. It has been shown that all possible operating conditions can be summarized with respect to the modifier concentration into three cases. These have been solved analytically by constructing the solution first in the hodograph plane, and then mapping it onto the physical plane using the method of characteristics. The peculiar properties of the derived hodograph plane were explained, and their impact on the pulse propagation for the three different cases has been elucidated. For the cases of intermediate adsorptivity of the modifier, the occurrence of solute peaks with infinitely high concentrations; that is, solute impulse, has been proven as well as the phenomena of double solute peaks. © 2005 American Institute of Chemical Engineers *AIChE J,* 52: 565–573, 2006
Keywords: chromatography (LC & SMB), mathematical modeling

Introduction

In many chromatographic applications, a modifier is added to the eluent since it allows the adjustment of the retention properties of the solutes over a wide range by regulating its concentration. In order to measure the retention as a function of the modifier concentration, the solute being dissolved in the so-called sample-solvent is injected into the eluent stream with varying modifier concentrations. If the modifier concentration in the sample-solvent is different from the one in the background mobile phase, the injection leads to two peaks traveling along the column: a solute peak and a positive or negative modifier perturbation. Interferences between these two peaks leads to peak deformation, double peaks, retention time distortion and other phenomena that have been investigated experimentally by several researchers.[1-7]

The objective of this work is to analyze in a general way the pulse propagation of a solute, whose retention depends on the

Correspondence concerning this article should be addressed to M. Morbidelli at massimo.morbidelli@chem.ethz.ch.

concentration of a modifier, in the cases where the concentration of the modifier in the injected pulse and in the background mobile phase is different.

In a previous article,[8] a mathematical analysis of the solute propagation was carried out by decoupling the modifier from the solute propagation. However, this type of analysis is sufficient only for simple situations, and does not allow for a satisfactory treatment of all possible cases. In this work, the problem of the pulse propagation is analyzed as a full-fledged binary problem, thus, allowing for a comprehensive treatment of all possible situations and highlighting a number of peculiar characteristics of this system, which might have a more general value and applicability.

Equilibrium model and method of characteristics

The equilibrium theory of chromatography is a powerful tool, since it allows to obtain explicit solutions and useful insights for a variety of chromatographic applications. It assumes, besides the common modeling simplifications like one-dimensional (1-D) flow, constant fluid velocity, and so on, that the mass transfer resistance and the axial dispersion in the column are negligible. More details about the modeling of chromatography can be found elsewhere.[9-11]

For the binary system treated in this work, where subscripts 1 and 2 denote the modifier and the solute, respectively, the material balance equations can be written in the frame of equilibrium theory as follows

$$\varepsilon \frac{\partial c_1}{\partial \tau} + (1-\varepsilon)\frac{\partial n_1}{\partial \tau} + \frac{\partial c_1}{\partial x} = 0 \tag{1}$$

$$\varepsilon \frac{\partial c_2}{\partial \tau} + (1-\varepsilon)\frac{\partial n_2}{\partial \tau} + \frac{\partial c_2}{\partial x} = 0 \tag{2}$$

where ε denotes the total column porosity, c_i and n_i the liquid and solid phase concentrations, respectively, $\tau = ut/(L\varepsilon)$ the dimensionless time, with u superficial velocity and L column length, and $x = z/L$ the dimensionless space coordinate. This system of equations has to be completed with the adsorption isotherms. A linear isotherm is assumed for the modifier, that is

$$n_1 = H_1 c_1 \tag{3}$$

The adsorption of the solute is also described by a linear isotherm, but the Henry constant H_2 depends on the modifier concentration according to

$$n_2 = H_2(c_1)c_2 \tag{4}$$

The Henry coefficient of the solute is assumed to decrease continuously with increasing modifier concentration,[8] that is

$$\frac{dH_2}{dc_1} = H_2'(c_1) < 0 \tag{5}$$

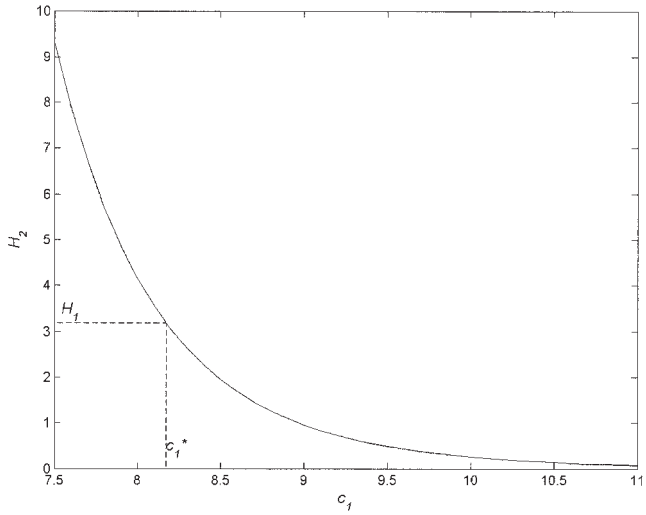

Figure 1. Henry constant of the solute H_2 as a function of the modifier concentration c_1 [g/l] ($H_2 = A(c_1\ [g/l])^B$ with $A = 8.43 \times 10^{11}$, $B = -12.52$ and $H_1 = 3.18$, data obtained from Melter et al. [12]).

for every c_1. The derivatives n_{ij} obtained by differentiating n_i with respect to c_j, are given by

$$\begin{aligned} n_{11} &= H_1 \\ n_{12} &= 0 \\ n_{22} &= H_2 \\ n_{21} &= H_2' c_2 \end{aligned} \tag{6}$$

In the framework of equilibrium theory, Eqs. 1 and 2 are solved with the method of characteristics, and are conveniently dealt with on the so-called hodograph plane, that is, the plane with coordinates $(c_2,\ c_1)$.[9,10] The characteristic directions in the hodograph plane, $\zeta = dc_1/dc_2$, can be calculated by solving the quadratic equation.[9,10]

$$n_{21}\zeta^2 - (n_{11} - n_{22})\zeta - n_{12} = 0 \tag{7}$$

This leads besides $\zeta = 0$ to the following solution

$$\zeta = \frac{H_1 - H_2}{H_2' c_2} \tag{8}$$

Let us define c_1^* by letting $H_1 = H_2(c_1^*)$ (see Figure 1); it is then clear that

i) $H_2 < H_1$ is equivalent to $c_1 > c_1^*$
ii) $H_2 > H_1$ is equivalent to $c_1 < c_1^*$

Let us denote the two solutions with $\zeta_+ > \zeta_-$; three cases can be distinguished $H_1 > H_2$, $H_1 < H_2$ and $H_1 = H_2$. Therefore

$$c_1 > c_1^* \Rightarrow \begin{cases} \zeta_+ = 0 \\ \zeta_- = \dfrac{H_1 - H_2}{H_2' c_2} \end{cases} \tag{9}$$

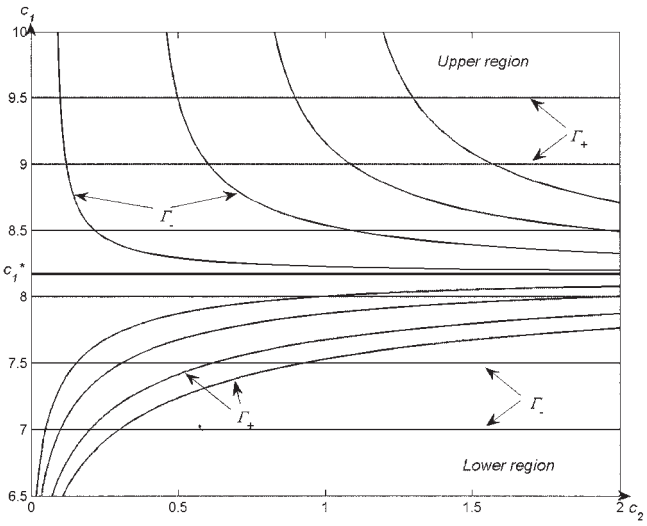

Figure 2. $\Gamma_\pm$ characteristics in the hodograph plane (c_1, c_2 [g/l], parameters as in Figure 1).

$$c_1 < c_1^* \Rightarrow \begin{cases} \zeta_+ = \dfrac{H_1 - H_2}{H_2' c_2} \\ \zeta_- = 0 \end{cases} \tag{10}$$

$$c_1 = c_1^* \Rightarrow \begin{cases} \zeta_+ = 0 \\ \zeta_- = 0 \end{cases} \tag{11}$$

From the first of Eq. 9, and the second of Eq. 10, it follows that the characteristics Γ_+ for $c_1 > c_1^*$ and Γ_- for $c_1 < c_1^*$ are horizontal lines, that is

$$c_1 = const \tag{12}$$

The Γ_+ for $c_1 < c_1^*$ and Γ_- for $c_1 > c_1^*$ can easily be determined by integrating the second of Eq. 9 or the first of Eq. 10 from an arbitrary point (c_1^0, c_2^0)

$$\frac{c_2}{c_2^0} = \frac{H_1 - H_2(c_1^0)}{H_1 - H_2(c_1)} \tag{13}$$

A typical plot of the $\Gamma_\pm$ characteristics in the hodograph plane is shown in Figure 2.

It is noteworthy that the hodograph plane is naturally divided into two distinct regions, that is, above and below the $c_1 = c_1^*$ characteristic, and that the role of the Γ_+ and Γ_- characteristics in the two regions is interchanged. This is a peculiar feature of this system and no other example of this kind has been reported in the literature.

It is worth mentioning that the part of the vertical axis above $c_1 = c_1^*$ is a Γ_-, whereas its portion below $c_1 = c_1^*$ is a Γ_+ (cf. Eq. 8). It is also clear from Eq. 13 that the Γ_+ and Γ_- in the lower and upper region, respectively, asymptotically approach the horizontal line $c_1 = c_1^*$ as $c_2 \to \infty$ and the y-axis as $c_2 \to 0$. Where the two characteristics, Γ_+ and Γ_-, merge together along the horizontal line $c_1 = c_1^*$, the system of partial differential equations becomes therefore parabolic. In the upper region ($c_1 > c_1^*$), the limiting Γ_-, that is, its vertical and horizontal asymptote, consists of the vertical axis above $c_1 = c_1^*$ and the horizontal line $c_1 = c_1^*$, whereas in the lower region ($c_1 < c_1^*$), the limiting Γ_+ consists of the vertical axis below $c_1 = c_1^*$ and the horizontal line $c_1 = c_1^*$.

According to the simple wave theory,[9,10] if the solution to equations 1 and 2 has its image on a Γ_- or Γ_+ in the hodograph plane, then the solution in the physical plane (x, τ) is constituted of a family of straight C_+ or C_- characteristics, respectively, whose slope is given by

$$\frac{d\tau}{dx} = \sigma_+ = 1 + \nu(n_{11} - n_{21}\zeta_+) \tag{14}$$

or

$$\frac{d\tau}{dx} = \sigma_- = 1 + \nu(n_{11} - n_{21}\zeta_-) \tag{15}$$

respectively, where $\nu = (1-\varepsilon)/\varepsilon$ is the phase ratio. From Eq. 6 and 9, therefore, we obtain for the case $c_1 > c_1^*$ (upper region) the following equations

$$\sigma_+ = 1 + \nu H_1 \tag{16}$$

$$\sigma_- = 1 + \nu H_2(c_1) \tag{17}$$

At this point it is important to note that c_1 remains constant along a Γ_+ and thus according to Eq. 17 also σ_- remains constant. On the other hand σ_+ is constant also along a Γ_-.

Likewise, from Eqs 6 and 10, in the case $c_1 < c_1^*$ (lower region) it follows that

$$\sigma_+ = 1 + \nu H_2(c_1) \tag{18}$$

$$\sigma_- = 1 + \nu H_1 \tag{19}$$

A similar argument as in the previous case can be made.

Since we are concerned with the propagation of pulses of solute and modifier, the initial and feed conditions can be written as follows

$$\begin{array}{lll} \text{At } \tau = 0, & c_1 = c_1^0 \text{ and } c_2 = c_2^0 & \\ \text{At } x = 0, & c_1 = c_1^F \text{ and } c_2 = c_2^F & \text{for } 0 < \tau < \tau_P \\ & c_1 = c_1^0 \text{ and } c_2 = c_2^0 & \text{for } \tau > \tau_P \end{array} \tag{20}$$

where τ_P denotes the duration of the pulse injection. This type of problem is also called a chromatographic cycle.

Initial and feed state in the same region of the hodograph plane

Here we shall consider the cases where the initial state ***0*** corresponding to (c_1^0, c_2^0), and the feed state ***F*** corresponding to (c_1^F, c_2^F) are located in the same region, that is, either in the upper or in the lower region, of the hodograph plane. It will always be assumed that $c_1^F < c_1^0$, since the opposite case can be easily treated accordingly and its analysis does not bring additional insights.[8] The two states ***0*** and ***F*** can, therefore, be

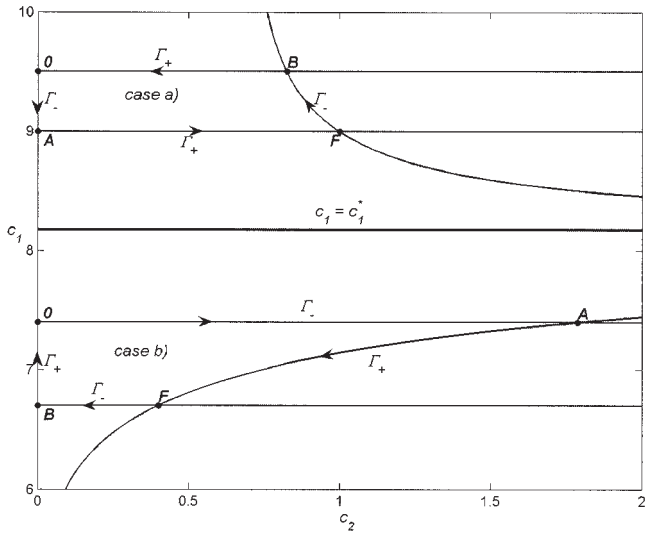

Figure 3. Solution in the hodograph plane, case (a) and case b.

assigned with respect to c_1 to one of the two cases (see Figure 3):

- Case (a): $c_1^0 > c_1^F = c_1^*$; hence, $H_2(c_1^0) < H_2(c_1^F) < H_1$
- Case (b): $c_1^* > c_1^0 > c_1^F$; hence $H_2(c_1^0) > H_2(c_1^F) > H_1$

Clearly, the injected pulse will always contain the solute, hence, $c_2^F > 0$, whereas for both cases $c_2^0 = 0$. The case with non vanishing c_2^0 will be treated in the next section. Here, we have piecewise constant initial and feed data containing two discontinuities, one at the origin and the other at the point $(0, \tau_P)$. This indicates that two separate Riemann problems associated with a quasilinear system of first-order differential equations are to be solved. According to the equilibrium theory, the solution of a Riemann problem has its image along Γ characteristics in the hodograph plane.[9, 10] In general, it will consist of two portions of characteristics, which are to be taken always in the sequence Γ_- - Γ_+ going from the state on the lefthand side of the discontinuity to the state on the righthand side of it.[9, 10] For the Riemann problem with a discontinuity at the origin, for instance, starting from the feed state ***F***, we must follow first the Γ_- passing through the point ***F*** and then switch to the Γ_+ going through the point ***0***.

Let us first consider case a) where the states ***0*** and ***F*** are in the upper region in Figure 3. For the sake of simplicity, we consider first the two Riemann problems independently and then we combine the two solutions, thus, obtaining the solution of the complete chromatographic cycle defined by equation 20. The Riemann problem associated to the discontinuity in $(0, \tau_P)$ corresponds to moving from state ***0*** (on the lefthand side in the physical plane) to state ***F*** (on the righthand side). The Riemann problem associated to the discontinuity in the origin corresponds to moving from ***F*** on the left to ***0*** on the right.

As shown in Figure 3, going from ***0*** to ***F*** via a Γ_- and a Γ_+ characteristics leads to the intermediate state ***A*** $(c_1^F, c_2 = 0)$ which is obtained as the intersection of the Γ_- characteristic going through ***0*** (that is, the c_1-axis) and the Γ_+ passing through ***F***.

The solution is constituted of three constant states, corresponding to each of the three points, ***0***, ***A***, and ***F***, which are separated by simple waves, as shown in the left hand side of Figure 4. In general, simple waves are constituted of all characteristics associated to the composition states between the two states on the two sides of the simple wave itself (states ***0*** and ***A*** or states ***A*** and ***F*** in this case). Since in this case, as discussed earlier with reference to Eqs. 16 and 17, all characteristics C_+ and C_- have the same slope in the Γ_- and Γ_+ simple waves, respectively, the simple waves reduce to a straight line with slope σ_+ and σ_- (see Figure 4). Therefore, there is a discontinuity between ***0*** and ***A*** and between ***A*** and ***F***. They are not self sharpening shocks,[9,10] but so-called contact discontinuities, and are typical of systems characterized by linear adsorption isotherms.

The second discontinuity in the initial data associated to case a) is from ***F*** to ***0***, and its propagation in the physical plane is illustrated in the righthand side of Figure 4. With reference to Figure 3, the new intermediate state ***B*** is defined, which is the intersection of the Γ_- passing through ***F***, and the Γ_+ going through ***0***. The solution in the physical plane can be constructed by following the same procedure as described for the previous discontinuity. Also, in this case the new constant state ***B*** is bounded by two contact discontinuities, and c_2^B is larger than zero, but smaller than the solute concentration in the pulse, c_2^F. Its value can be determined through equation 13 (note that $c_1^B = c_1^0$)

$$c_2^B = c_2^F \frac{H_1 - H_2(c_1^F)}{H_1 - H_2(c_1^0)} \tag{21}$$

Combining the results illustrated in the two parts of Figure 4 yields the complete solution of the chromatographic cycle defined by Eq. 20, as shown in Figure 5. Here, the C_+ and C_- characteristics emanating from the origin and from the point $(0, \tau_P)$, respectively, intersect at a point α (provided that $\tau_P < \nu(H_1 - H_2(c_1^F))$), from which a new Riemann problem with the states ***A*** and ***B*** on the left- and righthand side, respectively, has to be considered. With reference to Figure 3, states A and B are connected by a Γ- simple wave and then by a Γ_+ simple wave separated by the initial state ***0***; both simple waves are contact discontinuities. Beside the picture of the solution in the physical plane, Figure 5 shows also the corresponding concentration profiles of solute (solid line) and modifier (dashed line) at the column outlet.

The interaction between the two contact discontinuities allows the solute peak to be separated from the modifier peak.

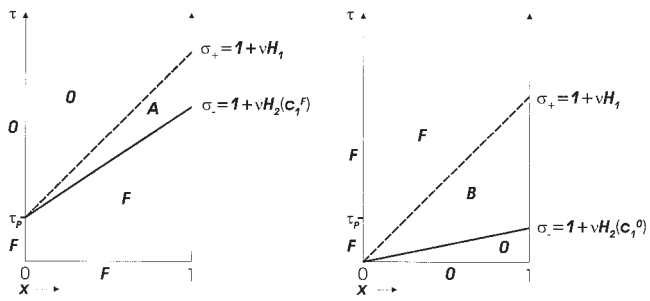

Figure 4. Solution in the physical plane, connecting state *0* to *F* (on the lefthand side), and state *F* to *0* (on the righthand side); case a.

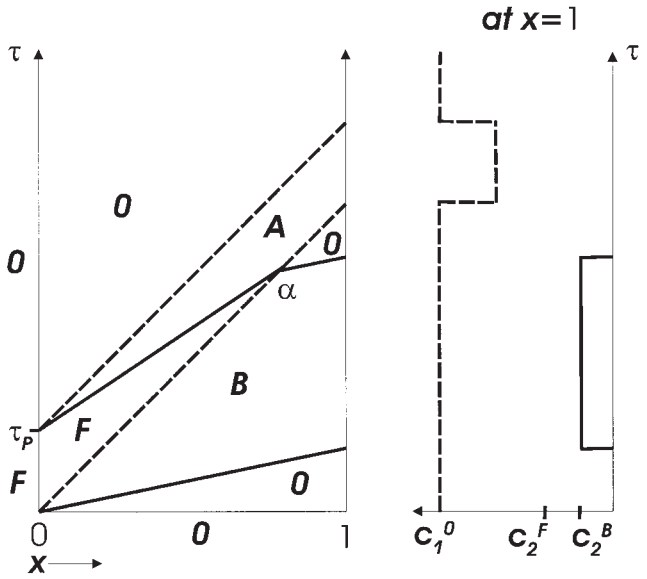

Figure 5. Complete solution in the physical plane and chromatogram at the exit, case a.

Solid line: solute, dashed line: modifier.

Clearly, the solute peak of concentration c_2^F has a higher propagation velocity than the modifier peak of concentration c_1^F, and it has even a higher velocity outside the modifier peak c_1^B. Therefore, the solute peak is eluted earlier than the modifier peak and it is broadened due to the interference with the modifier peak. The peak broadening leads obviously to a lower solute concentration, c_2^B, so as to satisfy the overall column mass balance (cf. Ströhlein et al.[8]).

Let us now consider case b), where all states are situated in the lower region of the hodograph plane because c_1^F, $c_1^0 < c_1^*$ (see Figure 3). As in case a), the state ***F*** is situated below and to the right with respect to state ***0***, which is on the c_1-axis. Connecting state ***0*** to ***F*** via Γ characteristics requires moving first along the horizontal Γ_- characteristic going through ***0***, and then along the Γ_+ characteristic going through ***F***. The intersection of these Γ_- and Γ_+ characteristics is the intermediate constant state ***A***, where the solute concentration c_2^A is higher than c_2^F, according to Eq. 13. The connection back from ***A*** to ***F***is obtained accordingly involving the new intermediate state ***B*** on the c_1 axis. The complete picture in the hodograph plane is shown in the lower part of Figure 3.

The lines separating the different constant states in the physical plane when going from ***0*** to ***F*** are shown on the lefthand side of Figure 6 and it is to be noted that the slopes of σ_+ and σ_- of the C_+ and C_- characteristics are this time given by equations 18 and 19, respectively, since c_1^F, $c_1^0 < c_1^*$. Here again, one may note that σ_+ (or σ_-) remains constant along ***0*** – ***A*** (or ***A*** – ***F***) of the hodograph plane and the discontinuity propagating along the C_+ (or C_-) characteristics is not a shock, but a contact discontinuity.

Using the corresponding plot for the connection ***F*** to ***0*** via ***B*** in the physical plane as shown on the righthand side of Figure 6, the complete picture of the chromatographic cycle in the physical plane can be developed as depicted in Figure 7. It is observed that the C_+ and C_- characteristics emanating from the origin and from point $(0, \tau_P)$, respectively, meet each other at

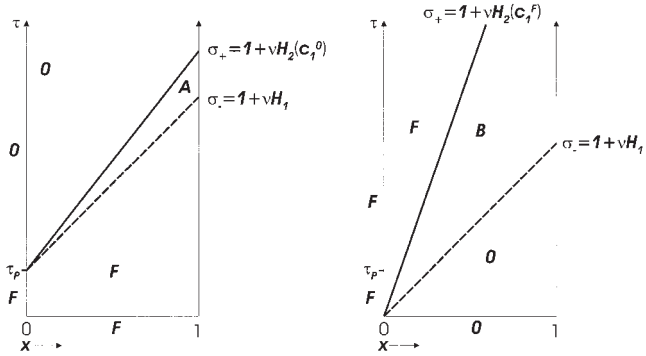

Figure 6. Solution in the physical plane, connecting state *0* to *F* (on the lefthand side), and state *F* to *0* (on the righthand side); case b.

point α to generate a new Riemann problem and to develop a new constant state ***0***. In this case the C_+ characteristics is refracted with a lower slope after the interaction because the slope σ_+ after the interaction is smaller than before.

Through the interaction between the two contact discontinuities, the solute and the modifier peaks separate and the former elutes later. Furthermore, the solute peak becomes narrower due to the interference with the modifier peak, hence the solute concentration c_2^A becomes higher than c_2^F, again in accordance with the overall column mass balance[8].

Initial and feed state in different regions of the hodograph plane

In this section we shall be concerned with the case where the initial state ***0*** is located in the upper region and the feed state ***F*** in the lower region, that is:

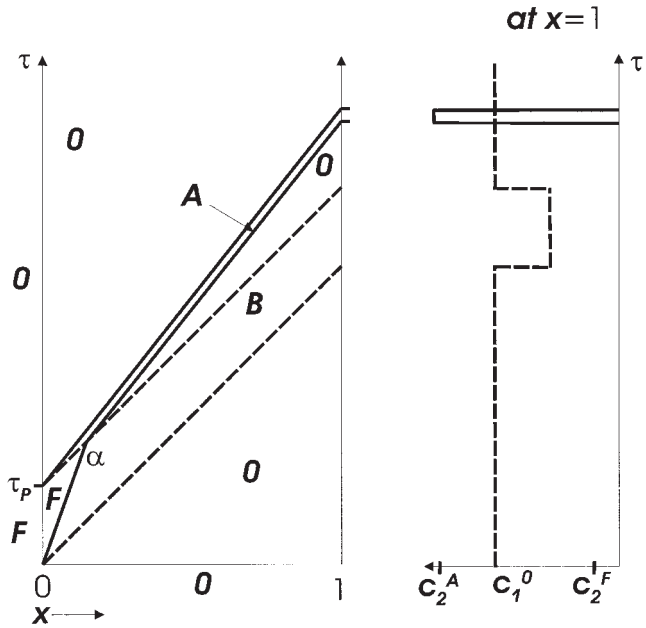

Figure 7. Complete solution in the physical plane and chromatogram at x = 1; case b.

Solid line: solute, dashed line: modifier.

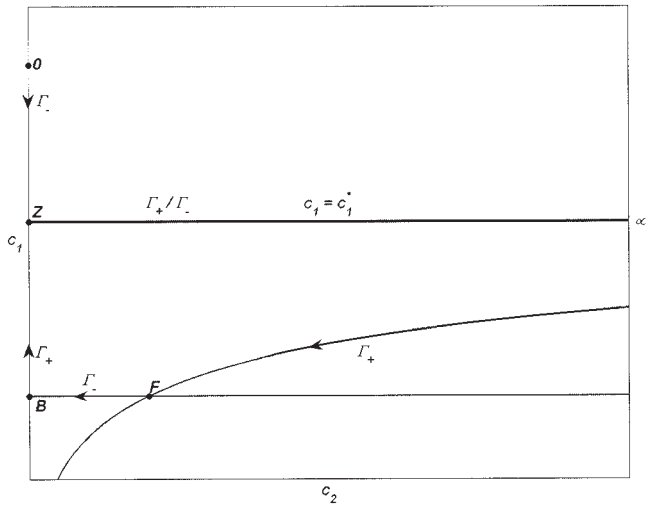

Figure 8. Solution in the hodograph plane; case c.

- Case (c): $c_1^0 > c_1^* > c_1^F$; hence, $H_2(c_1^0) < H_1 < H_2(c_1^F)$
- Moreover, we will consider the same case with nonvanishing c_2^0; that is,
- Case (d): $c_1^0 > c_1^*\, c_1^F;\ c_2^0 > 0$.

In these cases, the situation gets more complicated since the migration velocity of the modifier is intermediate between those of the solute at c_1^0 and at c_1^F. It was argued in the previous work[8] that the solute is accumulated at the end of the modifier peak. This peculiar behavior can be nicely elucidated by applying the hodograph plane analysis presented in this work.

Let us consider case (c), whose hodograph plane representation is shown in Figure 8, where the points ***0*** (c_1^0, 0), ***Z*** (c_1^*, 0), ***B*** (c_1^F, 0) and ***F*** (c_1^F, c_2^F) are highlighted. Going from ***F*** (on the left) to ***0*** (on the right) required moving along the Γ_- from ***F*** to ***B*** first, and then moving from ***B*** to ***0*** (through ***Z***) along the c_1 axis. The latter is allowed since the slope of the characteristics in the physical plane along the Γ_+ $\boldsymbol{B} \rightarrow \boldsymbol{Z}$ (Eq. 19), and along the Γ_- $\boldsymbol{Z} \rightarrow \boldsymbol{0}$ (Eq. 16) is the same, namely $1+\nu H_1$. The corresponding solution in the physical plane is illustrated in the righthand side of Figure 9, and is essentially the same as that of Figure 6 (righthand side). Going from 0 (on the left) to F (on the right), as in the case of the Riemann problem defined by equation 20 in $(0, \tau_P)$, is more challenging because the path ***0*** $\rightarrow$ ***Z*** $\rightarrow$ ***B*** $\rightarrow$ ***F*** is not allowed, since it would involve the wrong sequence of a Γ_+ simple wave (***Z*** $\rightarrow$ ***B***) followed by a Γ_- simple wave (***B*** $\rightarrow$ ***F***). The difficulty is solved by noting that point ***Z*** can be connected to ***F*** first through the horizontal characteristic $c_1 = c_1^*$ (whose corresponding characteristic in the physical plane has slope $1+\nu H_1$, as those belonging to the simple wave connecting ***0*** to ***Z***), and then through the Γ_+ characteristic going through ***F*** (see Figure 8), along which again the characteristics in the physical plane have slope $1+\nu H_1$, according to Eq.19. This rather special situation leads to a solution in the physical plane (see lefthand side of Figure 9), where the states ***0*** and ***F*** are separated by a contact discontinuity with slope $1+\nu H_1$, which is the projection on the (x, τ) plane of the characteristics propagating all the competition states belonging to the path ***0*** $\rightarrow$ ***Z*** $\rightarrow \infty \rightarrow$ ***F***. When the two solutions shown in Figure 9 are brought together, thus, yielding the solution of the complete chromatographic cycle of case c, the final result illustrated in Figure 10 is obtained.

It is clear that the contact discontinuities between states ***0*** and ***F*** and between states ***F*** and ***B*** intersect at point α. On its lefthand side, the solution has its image in the hodograph plane along the path ***0*** $\rightarrow$ ***Z*** $\rightarrow \infty \rightarrow$ ***F*** $\rightarrow$ ***B*** $\rightarrow$ ***Z*** $\rightarrow$ ***0***. Beyond point α, the states ***0*** and ***B*** are to be connected through the path ***0*** $\rightarrow$ ***Z*** $\rightarrow \infty \rightarrow$ ***Z*** $\rightarrow$ ***B***, all corresponding characteristics in the physical plane having slope $1+\nu H_1$. This indicates that the injected pulse of the solute has been focused on the trailing edge of the modifier pulse, and leaves the column as an infinite impulse in the frame of the equilibrium theory approximation (see the outlet composition profile in Figure 10). Such a peculiar result has been observed experimentally, as well as through simulations[8], and it is explained here rigorously, for the first time.

As a variation of case (c), let us consider case (d), where the bed in its initial state, as well as the eluent contain an amount of solute, so that point ***0*** is located as shown in Figure 11.

The transition between state ***0*** (on the left) and state ***F*** (on the right) yields the same result as in the previous case c as shown in Figure 12 (lefthand side). The transition from ***F*** (on the left) to ***0*** (on the right) follows the hodograph plane path ***F*** $\rightarrow$ ***B*** $\rightarrow$ ***Z*** $\rightarrow$ ***A*** $\rightarrow$ ***0*** and involves three contact discontinuities as shown in the righthand side of Figure 12. The solution of the

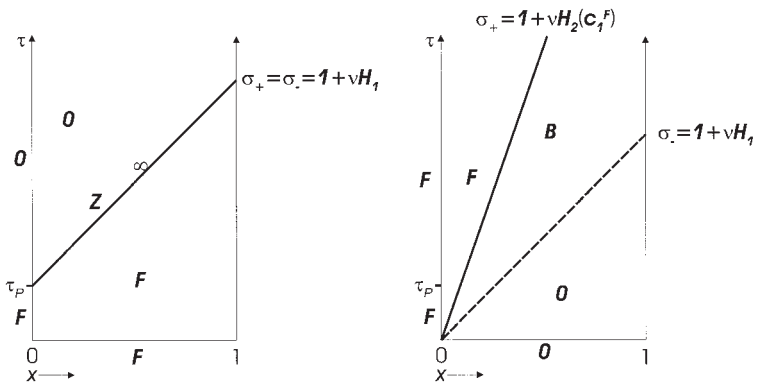

Figure 9. Solution in the physical plane, connecting state *0* to *F* (on the left-hand side), and state *F* to *0* (on the righthand side); case c.

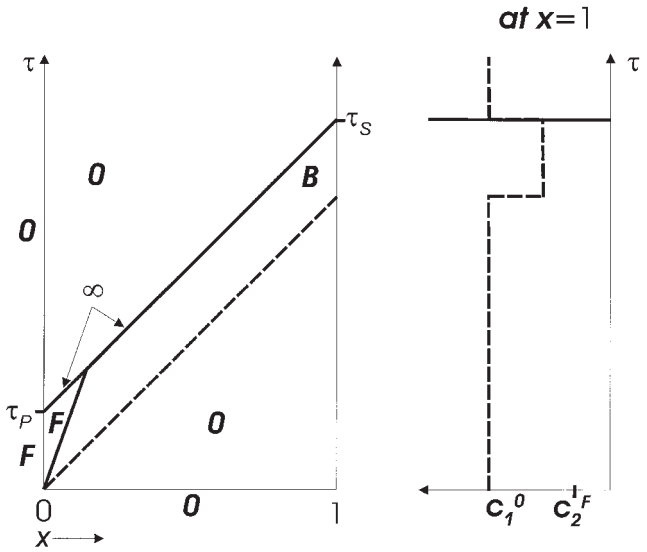

Figure 10. Complete solution in the physical plane and chromatogram at x = 1; case c.

Solid line: solute, dashed line: modifier

complete chromatographic cycle can be obtained accordingly and it is shown in Figure 13.

From a chromatographic viewpoint, it is worth noting that the solute is not present in the time interval when states ***A*** and ***B*** are eluted, whereas it comes out as an infinite impulse at time τ_S. The consequences of this phenomenon for chromatographic separations have been discussed earlier.[8]

Stepwise gradient chromatography

A final example highlights the effectiveness of the methods developed earlier to understand the behavior of more complex chromatographic cycles. With reference to Figure 14, let us consider a column that is initially saturated with mobile phase at a low modifier content c_1^0 (state ***0***). The solute is injected between *0* and τ_P at a concentration c_2^F. The modifier concentration (state ***F***) in the injected pulse between *0* and $\tau_P/2$ is

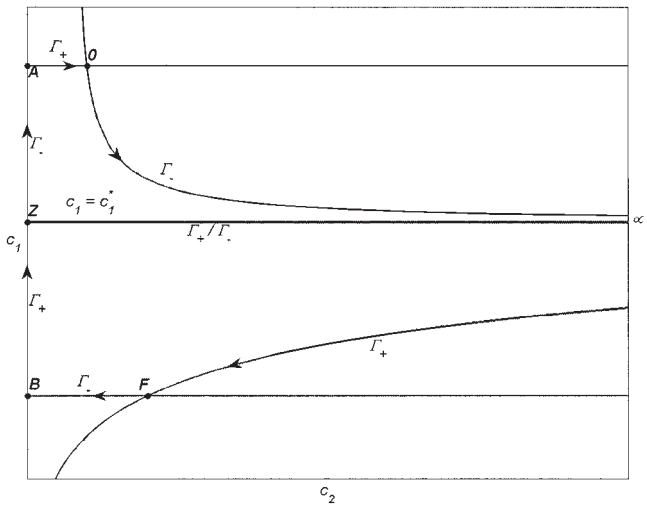

Figure 11. Solution in the hodograph plane; case d.

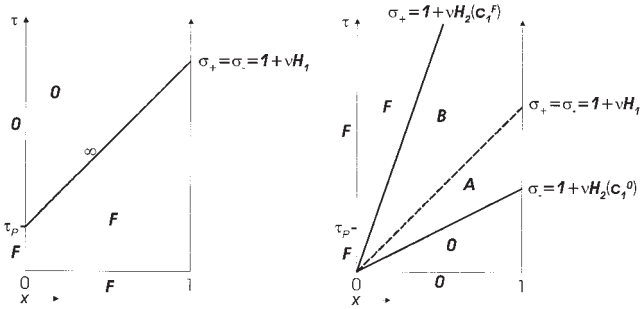

Figure 12: Solution in the physical plane, connecting state *0* to *F* (on the lefthand side), and state *F* to *0* (on the righthand side); case d.

larger than the initial value (state ***0***), and it increases further between $\tau_P/2$ and τ_P (state ***F′***). It is worth pointing out that ***F*** and ***F′*** are below and above the line $c_1 = c_1^*$, respectively. Finally, the solute is eluted by feeding the solvent with modifier at the highest concentration (state ***0′***).

This can be viewed as a stepwise implementation of gradient chromatography. Based on the examples discussed earlier it is rather clear that state ***0′*** can be connected to state ***0*** in the hodograph plane through the sequence $\boldsymbol{0'} \rightarrow \boldsymbol{A} \rightarrow \boldsymbol{F'} \rightarrow \infty \rightarrow \boldsymbol{F} \rightarrow \boldsymbol{B} \rightarrow \boldsymbol{0}$, each state being separated from the next by a line as illustrated in the hodograph plane and in the physical plane in Figures 14 and 15, respectively. The contact discontinuities between ***0′*** and ***A***, between ***F′*** and ∞, between ∞ and ***F***, and between ***B*** and ***0***, have slope $1+\nu H_1$. With respect to the other two contact discontinuities, the one $\boldsymbol{A} \rightarrow \boldsymbol{F'}$ has slope $1+\nu H_2(c_1^{F'})$, which is smaller than $1+\nu H_1$, and the other $\boldsymbol{F} \rightarrow \boldsymbol{B}$ has slope $1+\nu H_2(c_1^F)$, which is larger than $1+\nu H_1$. It is worth noting that the contact discontinuities between ***F′*** and ∞ and between ∞ and ***F*** are the images of all concentrations on the Γ_- and Γ_+ characteristics connecting states ***F′*** and ∞ and states ∞ and ***F***, through the point (c_1', ∞), in the hodograph plane.

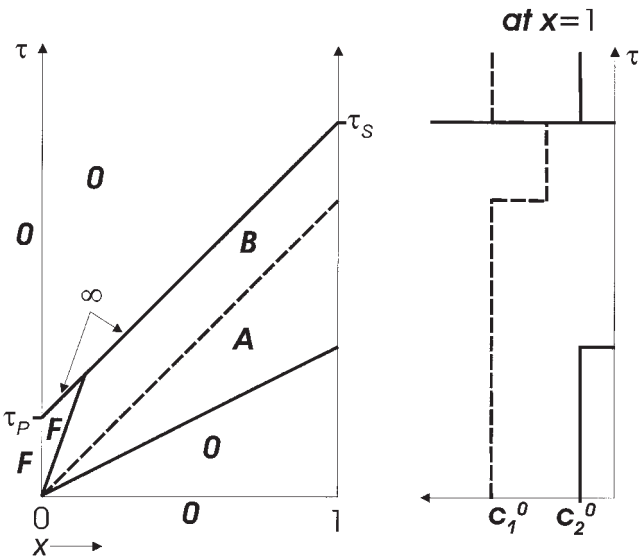

Figure 13. Complete solution in the physical plane and chromatogram, case d.

Solid line: solute, dashed line: modifier.

As shown in Figure 15, the two contact discontinuities between $\boldsymbol{A}$ and $\boldsymbol{F}'$ and between $\boldsymbol{F}$ and $\boldsymbol{B}$ mentioned previously intersect the one between $\boldsymbol{F}'$ and $\boldsymbol{F}$, that is, the one emanating from point $(0, \tau_P/2)$ with slope $1+\nu H_1$, at point α and β. On the righthand side of the second intersection, states $\boldsymbol{0}'$ and $\boldsymbol{0}$ are connected through the path $\boldsymbol{0}' \rightarrow \boldsymbol{A} \rightarrow \boldsymbol{Z} \rightarrow \infty \rightarrow \boldsymbol{Z} \rightarrow \boldsymbol{B} \rightarrow \boldsymbol{0}$; and the three remaining contact discontinuities have the same slope as $1+\nu H_1$. It is then apparent that the solute fed during the finite time period 0 to τ_P has been focused to give rise to a solute impulse and leaves the column as an impulse at the time $\tau_P/2+1+\nu H_1$, as shown in the righthand side diagram of Figure 15.

Such a phenomenon has been observed with pH gradient in high-performance cation-exchange column, where it has been called "chromatofocusing" [13-15] and also with temperature gradients.[16]

Discussion and Conclusions

Although the chosen isotherm models are very simple, the characteristics in the hodograph plane, that is, the plane of the solute and the modifier concentrations, show very peculiar properties, particularly the division of the hodograph plane in two distinct regions and the inversion of the Γ_+ and Γ_- characteristics between these two regions. The hodograph plane is divided by a horizontal line, which is located at the modifier concentration, for which the Henry constant of the solute is equal to the Henry constant of the modifier.

If the states $\boldsymbol{0}$ and $\boldsymbol{F}$ corresponding to the fresh bed or pure solvent and the feed, respectively, are located in the same region in the hodograph plane, peak deformation, that is, peak broadening or sharpening, occurs due to the interaction between the modifier and the solute pulses. The change in the solute concentration of the deformed peaks can be explained and calculated by tracing the Γ characteristics in the hodograph plane.

If the two states $\boldsymbol{0}$ and $\boldsymbol{F}$ are located in different regions of the hodograph plane, the appropriate connection via the Γ characteristics passes a state with infinite solute concentration, which is situated on the horizontal line dividing the two regions in the hodograph plane. Along this line the Henry constants of modifier and solute are the same. Therefore, the solute pulse appears as an impulse at the end of the modifier pulse.

When a solute pulse is injected along with stepwise increasing modifier concentrations, where the lower and the higher modifier concentrations are situated in the lower and upper region of the hodograph plane, it is elucidated that the interaction between the solute pulse and the modifier pulse gives rise to the focusing of solute to an impulse, which is equivalent to the chromatofocusing with pH gradient.

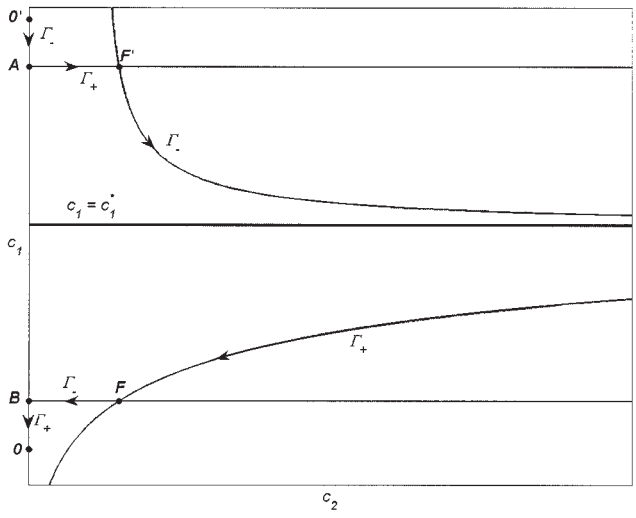

Figure 14. Solution in the hodograph plane, case e.

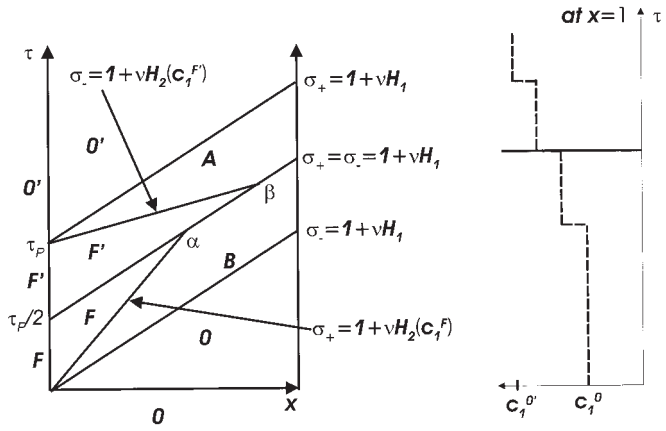

Figure 15. Complete solution in the physical plane and chromatogram, case e.

Solid line: solute, dashed line: modifier

Notation

c_i = liquid phase concentration of component i
H_i = Henry constant of component i
L = column length
n_i = solid phase concentration of component i
n_{ij} = derivative of n_i with respect to c_j
u = superficial velocity in column
t = time
$x = z/L$ = dimensionless space coordinate
z = space coordinate

Greek symbols

ε = total column porosity
Γ = characteristic line in the hodograph plane
$\zeta = dc_1/dc_2$ = characteristic direction in the hodograph plane
$\tau = ut/(L\varepsilon)$ = dimensionless time

Subscripts

1 = modifier
2 = solute

Literature Cited

1. Fornstedt T, Guiochon G. Comparison between experimental and theoretical profiles of high concentration elution bands and large system peaks in non-linear chromatography. *Analytical Chem.* 1994; 66:2686-2693.
2. Golshan-Shirazi S, Guiochon G. Theoretical study of system peaks in linear chromatography. *Analytical Chem.* 1990;62:923-932.
3. Golshan-Shirazi S, Guiochon G. Theorectical study of system peaks and elution profiles of high concentration bands of binary mixtures eluted by a binary eluent containing a strongly retained additive. *Analytical Chem.* 1989;61:2373-2380.
4. Feng W, Zhu X, Zhang L, Geng X. Retention behaviour of proteins

under conditions of column overload in hydrophobic interaction chromatography. *J of Chromatography A*. 1996;729:43-47.
5. Williams KJ, Li Wan Po A, Irwin WJ. Sample-solvent-induced peak broadening in the reversed-phase high-performance liquid chromatography of Aspirin and related analgesics. *J of Chromatography*. 1980; 194:217-223.
6. Vukmanic D, Chiba M. Effect of organic solvents in sample solutions and injection volumes on chromatographic peak profiles of analytes in reversed-phase high-performance liquid chromaography. *J of Chromatography*. 1989;483:189-196.
7. Jandera P, Guiochon G. Effect of the sample solvent on band profiles in preparative liquid chromatography using non-aqueous reversed-phase high-performance liquid chromatography. *J of Chromatography*. 1991;588:1-14.
8. Ströhlein G, Mazzotti M, Morbidelli M. Analysis of sample-solvent induced modifier-solute peak interactions in biochromatography using equilibrium theory and detailed simulations. *J of Chromatography A*. 2005;1091:60-71.
9. Rhee H-K, Aris R, Amundson NR. First-order partial differential equations, volume 1: theory and application of single equations. New York: Dover Publications; 2001.
10. Rhee H-K, Aris R, Amundson NR. First-order partial differential equations, volume 2: theory and application of hyperbolic systems of quasilinear equations. New York: Dover Publications; 2001.
11. Guiochon G, Golshan-Shirazi S, Katti AM. Fundamentals of preparative and nonlinear chromatography. Boston: Academic Press; 1994.
12. Melter L, Aumann L, Ströhlein G, Mazzotti M, Morbidelli M. Adsorption Properties of Monoclonal Antibody Variants in Analytical and Preparative Ion-Exchange Chromatography. 18th *International Symposium on Preparative Chromatography & Related Separation Techniques*, PA:Philadelphia; 2005.
13. Frey DD, Barnes A, Strong J. Numerical studies of multicomponent chromatography using pH gradients, *AIChE J*. 1995;41:1171-1183.
14. Frey DD. Local-equilibrium behavior of retained pH and ionic strength gradients in preparative chromatography. *Biotechnol Prog*. 1996;12: 65-72.
15. Kang X, Frey DD. High-performance cation-exchange chromatofocusing of proteins, *J of Chromatography A*. 2003;991:117-128.
16. Kim JK, Natarajan G, Wankat PC. Focusing in liquid thermal adsorption systems, *Adsorption-J of the Intl Adsorption Soc*. 2003:92:117-123.

Manuscript received Feb. 28, 2005, and revision Jun. 9, 2005.